C. R. Physique 17 (2016) 447–454

Contents lists available at ScienceDirect

Comptes Rendus Physique

www.sciencedirect.com

Condensed matter physics in the 21st century: The legacy of Jacques Friedel

The longevity of Jacques Friedel's model of the virtual bound state

La longévité du modèle d'état lié virtuel de Jacques Friedel

Peter M. Levy [a,*], Albert Fert [b,c]

[a] *Department of Physics, New York University, 4 Washington Place, New York, NY 10003, USA*
[b] *Unité mixte de physique CNRS/Thales, 91767, Palaiseau, France*
[c] *Université Paris-Sud, 91405 Orsay cedex, France*

ARTICLE INFO

Article history:
Available online 21 December 2015

Keywords:
Virtual bound state (vbs)
Phase shifts
Impurity scattering
Spin Hall effect
Dzyaloshinsky–Moriya Interaction (DMI)
Skew scattering

Mots-clés :
Magnétisme
Conduction électrique
Impuretés

ABSTRACT

We illustrate the continuing pertinence of Friedel's model of the virtual bound state to describe electron scattering in metals. This model has been applied to such disparate studies as the chirality of spin interactions in metals, and the spin Hall effect caused by scattering from impurities with spin–orbit coupling.

RÉSUMÉ

Nous illustrons la pertinence toujours actuelle du modèle de l'état lié de Friedel pour décrire la diffusion des électrons dans les métaux. Ce modèle a été appliqué à des problèmes aussi différentes que la chiralité des interactions de spin dans les métaux ou l'effet Hall de spin causé par la diffusion d'impuretés avec couplage spin–orbite.

1. Introduction

Many phenomena in solids involve the scattering of conduction electrons by substitutional impurities. During his doctoral thesis work with Neville Mott, Jacques Friedel studied the distribution of electrons around impurities in metals, and developed a method of virtual bound states [vbs] to describe the scattering of conduction electrons by the localized states of impurities [1]. It is based on describing scattering by a central impurity in terms of phase shifts of the incoming wave, and has been applied to a myriad of problems. The hybridization of the local states with the conduction electron states produces a broadening in the energy of the states; this is known as a vbs. When the energy of the localized state is close to the Fermi level, they affect electron transport. In the immediate vicinity of the impurity, the wave function is dominated by that of the local state; outside a range of the order of 1 nm, the wave function is that of a phase-shifted plane wave. These phase shifts are the signature of impurity scattering and affect electron transport in metals.

* Corresponding author.
E-mail address: levy@nyu.edu (P.M. Levy).

http://dx.doi.org/10.1016/j.crhy.2015.12.011

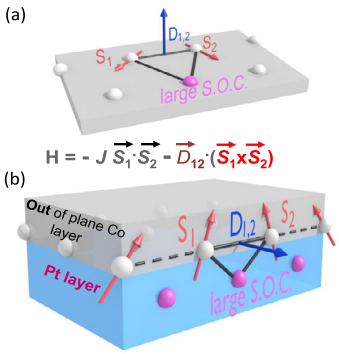

Fig. 1. (a) Triangular geometry that gives rise to DMI between the two atomic spins neighboring a nonmagnetic atom with large spin–orbit interaction. (b) A pair of atomic spins at the interface of a magnetic film with a metallic layer with large spin–orbit coupling in a noncentrosymmetric environment. Both figures are taken from Ref. [13].

To underscore the current use of Friedel's concept of a vbs, we focus on two phenomena: the spin Hall effect [SHE] due to scattering by impurities, and the chirality of exchange interactions between spins in disordered alloys or at the interface of magnetic films. Both phenomena rely on spin–orbit coupling [SOC]; hence a vbs model with orbit-dependent phase shifts is the appropriate method to describe spin–orbit split localized states in metals. The SHE induced by impurities relies on the phase shifts induced by nonmagnetic impurities that have spin–orbit coupled orbitals, while the chirality of indirect exchange arises when the phase shifted vbs's interact with neighboring local moments. The chirality arises from the character of the vbs close, of the order of 1–2 nm, to the local moments sensed at a distance through phase-shifted waves.

In the past five years there has been a renewed interest in the spin Hall effect as a source for converting charge into spin currents, e.g., the works by Mertig et al. [2], Maekawa et al. [3], as well as ours [4]. In all of these treatments, the scattering of conduction electrons by impurities that produce this effect is related to phase shifts that are determined from ab-initio calculations. In another vein, we studied [5] the anisotropy induced by ternary impurities, e.g., Pt, on the coupling between spins, Mn impurities, in metals such as Cu. In this work we first determined the scattering of conduction electrons by the impurities with strong spin–orbit coupling; subsequently the distorted waves emanating from the impurity interact with local moments at some distance from the center. The indirect coupling of two such moments interacting with the distorted waves is anisotropic; spin–orbit coupling makes coupling sensitive to the coordinates of the moments relative to the central scatterer. In the following, we review the role of phase shift analyses in conjunction with virtual bound states in determining these effects. This picture, that was first worked out for disordered alloys with low local symmetry, has been extended to situations in which inversion symmetry is broken for spins at the interface of a magnetic film. The resulting chiral interactions of the Dzyaloshinsky–Moriya type (DMI) are at the origin of the magnetic skyrmions in thin magnetic films deposited on a metal with large SOC [6].

Our article is limited to the application of the vbs model to the calculation of the SHE and the DMI. However, we point out that other concepts introduced by Friedel a long time ago are fashionable today, e.g., in the extensions of the Friedel oscillations concept to the situation where Rashba surface interactions give rise to skyrmionic spin oscillations [7].

2. Dzyaloshinsky–Moriya exchange interaction (DMI)

2.1. DMI in disordered magnetic alloys (spin glasses)

The interaction between local moments in metals, e.g., in CuMn spin glasses, is usually of the Ruderman–Kittel–Kasuya–Yosida (RKKY) type and isotropic, i.e., of the form $S_1 \cdot S_2$; however, it was found that the addition of nonmagnetic impurities with strong spin–orbit coupling (Au, Pt) sharply increases the anisotropy field that maintains the remanent magnetization in the direction of the initial applied field. In other words, by adding ternary impurities such as Pt, the local moments are harder to rotate, i.e. the anisotropic energy increases. At first, it was thought that the interaction between moments develop a pseudo dipole–dipole anisotropy. The surprising discovery was that it was primarily of the Dzyaloshinsky–Moriya (DM) form $D \cdot S_1 \times S_2$. The method used by us to find this relied on Friedel's description of localized states in metals, i.e., the vbs [5]; here we outline the method used.

The RKKY interaction is based on the calculation of the shift in the ground-state energy of a gas of conduction electrons interacting with two localized spins. Here we add a spin–orbit interaction on the site of a neighboring nonmagnetic impurity at $R = 0$ (see Fig. 1a) and therefore consider the following perturbing potential of the electron gas:

$$V = -\Gamma\delta(r - R_A)s \cdot S_A - \Gamma'\delta(r - R_B)s \cdot S_B + \lambda(r)l \cdot s \tag{1}$$

On the site of a nonmagnetic transition-metal impurity, the spin–orbit coupling of a conduction electron is considerably enhanced because the admixture of the impurity d states into the conduction band allows the conduction electrons to

experience the strong spin–orbit forces of the d states. In the virtual-bound-state model [8], the admixture of the atomic d states ψ_{2m} with plane waves is written as

$$\varphi_{\vec{k}} = \exp(i\vec{k}\cdot\vec{r}) + \exp(i\eta_2)\sin\eta_2 \frac{\langle d \mid V_0 \mid k\rangle}{\Delta} \sum_{m=-2}^{2} Y^*_{2m}(\hat{k})\psi_{2m}(\vec{r}) + \ldots \tag{2}$$

for electrons in the immediate region about the transition-metal impurity ($\vec{R} = 0$). In the region of large R, the wave function is written as

$$\varphi_{\vec{k}} = \exp(i\vec{k}\cdot\vec{r}) + 4\pi\exp(i\eta_2)\sin\eta_2 (e^{ikr}/kr) \sum_{m=-2}^{2} Y^*_{2m}(\hat{k})Y_{2m}(\vec{r}) \tag{3}$$

where Δ is the half-width of the virtual bound state and η_2 is the phase shift of the $l = 2$ partial waves. The phase shift at the Fermi level is related to the number Z_d of d electrons by the Friedel rule

$$\eta_2(E_F) = (\pi/10)Z_d \tag{4}$$

and the matrix element $\langle d \mid V_0 \mid k\rangle$ is related to the density of states for one spin direction at the Fermi level $N(E_F)$ by the relation [8]

$$|\langle d \mid V_0 \mid k\rangle|^2 = 4\Delta/N(E_F). \tag{5}$$

The lowest-order correction term to the ground-state energy due to the perturbation in Eq. (1) in which all three scattering centers appear is [9]

$$E^{(3)} = (\frac{1}{8\pi^3})^3 P \int_{k_1 \le k_F} d^3k_1 \int d^3k_2 \int d^3k_3 \left[\frac{1}{(E_1 - E_2)(E_1 - E_3)} - \frac{\pi^2}{3}\delta(E_2 - E_1)\delta(E_3 - E_2)\right] \times Tr_\sigma V_{\vec{k}_1\vec{k}_2} V_{\vec{k}_2\vec{k}_3} V_{\vec{k}_3\vec{k}_1} V_{\vec{k}_1\vec{k}_2} \tag{6}$$

where P denotes the principal part of the integral. In the systems to which we apply the perturbation in Eq. (1), the magnetic ions at $\vec{R}_A$ and $\vec{R}_B$ are far from the nonmagnetic impurity ($R_\alpha \sim 10$ Å). Therefore, to calculate the matrix elements of the exchange terms Γ in the perturbation in Eq. (1), we use the form of the wave function at large r, Eq. (3), while for the spin–orbit coupling term we use the form appropriate for small r, Eq. (2) inasmuch as it is placed at the origin in coordinate space in our calculation. The trace over the conduction-electron spin states that enter Eq. (6) is

$$Tr_\sigma(\vec{S}_A\cdot\vec{s})(\vec{s})(\vec{S}_B\cdot\vec{s}) = -(i/4)(\vec{S}_A\times\vec{S}_B) \tag{7}$$

After performing the integrations in Eq. (6), we finally obtain the leading term (in $1/R$) to the energy, which is trilinear in the three parts of the perturbation V [10],

$$H_{DM} = -V_1 \frac{\sin[k_F(R_A + R_B + R_{AB}) + (\pi/10)Z_d]\hat{R}_A\cdot\hat{R}_B}{R_A R_B R_{AB}} (\hat{R}_A\times\hat{R}_B)\cdot(\vec{S}_A\times\vec{S}_B) \tag{8}$$

with

$$V_1 = (135\pi/32)(\lambda_d\Gamma^2/E_F^2k_F^3)\sin[(\pi/10)Z_d] \tag{9}$$

Here R_A, R_B and R_{AB} are the lengths of the three sides of the triangle formed by the ions at A, B, and the spin–orbit center at the origin, λ_d is the spin–orbit coupling constant for a d electron and we have assumed one conduction electron per atom of the metal. Other anisotropic terms appear in higher-order perturbation terms, but they are proportional to $(\lambda_d/E_F)^n$, with $n \ge 2$, and we can neglect them. This derivation demonstrates that both the local as well as the phase shifted characters of the vbs describe the induced chiral anisotropy of the exchange interaction.

Summarizing, the ternary impurities act in such a way as to induce locally a spin–orbit coupling in the conduction electrons. When Mn magnetic moments interact with these modified conduction-electron states, the resultant magnetic coupling contains chiral terms whose magnitudes are sufficiently large to explain the anisotropy energies experimentally observed.

2.2. DMI at interfaces of magnetic films

The DMI's that occur in spin glasses (see preceding section) are due to spin–orbit interactions in the absence of inversion symmetry; for example, they arise for the situation shown in Fig. 1a with two magnetic atoms and a nonmagnetic atom with large spin–orbit coupling. This picture has been extended [11] to the situation shown in Fig. 1b with an interface between a magnetic layer (Co) and a layer of heavy metal with large spin–orbit coupling (Pt). The inversion symmetry is broken by the presence of the interface. With Pt atoms only below the interface, the DMI induced by the corresponding Co–Co–Pt

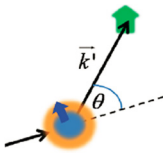

Fig. 2. Schematic representation of the asymmetry between left and right hand scattering called skew scattering.

triangles is not cancelled by the DMI that would be created if there were also Pt atoms above the interface. The existence of a large DMI at interface of magnetic films with nonmagnetic heavy metals as Pt, Ir, etc., has been now confirmed by ab-initio calculations [12]. These large interface DMI's are extensively studied today as they give rise to interesting chiral spin textures such as magnetic skyrmions and chiral magnetic domain walls. Magnetic skyrmions are topologically protected solitons that can be moved like nano-particles; they are very promising information carriers in ultra-dense memory, and as logic elements in spintronic devices [13]. Interfacial DMI's also stabilize Néel magnetic domain walls of a given chirality that are also promising for spintronic devices as they can be moved at very high speed by the SHE [14].

3. Spin Hall effect

The spin Hall effect consists of the appearance of spin accumulation on the lateral surfaces of a sample carrying electric current, or of a transverse spin current. It was first predicted by Dyakonov and Perel in 1971 [15], but it took about 35 years to realize it in the form it is known today. The term "Spin Hall Effect" was introduced by Hirsch in 1999. It is similar to the ordinary Hall effect, where charges of opposite sign build up at the transverse boundaries to compensate for the Lorentz force acting on the charge carriers in the sample due to a magnetic field. In contrast, no magnetic field is needed for the SHE; it belongs to the same family as the anomalous or extraordinary Hall effect, known in ferromagnets, which also originates from spin–orbit interaction. Indeed as far back as 1981 Fert et al. [16] showed that by first adding Mn magnetic impurities to Cu in order to create an imbalance in the number of up and down electron spins of the current and then introducing non-magnetic impurities with spin–orbit coupling, he was able to demonstrate that the transverse Hall effect is affected by the skew scattering of polarized currents.

With the advent of spintronics, the SHE has been found to be an efficient tool for the conversion of a charge current into a spin current; also, it is effective for the switching of a nanomagnet and the displacement of a domain wall. For impurity-induced spin Hall effects, two mechanisms related to the SOC contribute: the skew scattering and the scattering with side-jump [4]. Both mechanisms are involved in the anomalous Hall effect (AHE) of the ferromagnetic metals, have been extensively developed by different approaches [2–4]. Here we describe our approach of using Friedel's model of the vbs with a view to determining the scattering that produces the transverse spin currents.

3.1. Skew scattering

Skew scattering can be described as scattering which is asymmetric between the scattering probabilities to the right and left of a scattering center; see Fig. 2. The contribution of skew scattering to the AHE was first derived by Fert by using the transparent formula [16],

$$\rho_H^{\text{skew}}\,|_{\text{Fert}} = -\left(\frac{\hbar}{8\pi^3 ne}\right)^2 \int \left(-\frac{\partial f^0}{\partial \varepsilon_k}\right)(\vec{k}\cdot\hat{x})(\vec{k}'\cdot\hat{y}) W_{\text{antisym}}(\mathbf{k}\pm \rightarrow \mathbf{k}'\pm)\,\mathrm{d}^3k\,\mathrm{d}^3k' \tag{10}$$

where ϱ_H^{skew} represents the transverse resistivity ρ_{yx}^{skew}. To evaluate Fert's formula, we use the antisymmetric part of the transition probability,

$$W(\mathbf{k}\sigma \rightarrow \mathbf{k}'\sigma') = \frac{2\pi N_i}{\hbar}\left|T(\mathbf{k}\sigma \rightarrow \mathbf{k}'\sigma')\right|^2 \delta(\varepsilon_{k\sigma} - \varepsilon_{k'\sigma'}) = \frac{2\pi N_i}{\hbar}\left|T_{\mathbf{k}'\sigma',\mathbf{k}\sigma}\right|^2 \delta(\varepsilon_{k\sigma} - \varepsilon_{k'\sigma'}) \tag{11}$$

Here we have introduced the T matrix for the scattering from impurities [17] and retained only the combinations that are antisymmetric when interchanging k and k' inasmuch as this is needed for finding effects transverse to the current. We find,

$$W_{\text{antisym}}(\mathbf{k}\sigma \rightarrow \mathbf{k}'\sigma) = \frac{2\pi N_i}{\hbar}\delta(\varepsilon_{k'\sigma} - \varepsilon_{k\sigma})\left\{T^{\dagger}_{\text{antisym}} T_{\text{sym}} + T_{\text{antisym}} T^{\dagger}_{\text{sym}}\right\} \tag{12}$$

and use $T^{\text{s-o}}_{\mathbf{k}'\sigma',\mathbf{k}\sigma}$, for the antisymmetric scattering due to SOC. To illustrate how we relate the T matrix to phase shifts, we follow the recent work we presented on the spin Hall effect induced by Bi impurities in Cu [4].

The T matrix for scattering off a localized p state, at the Fermi energy, is found by following the derivation outlined in [21] which focused on scattering off 4f states. The two differences are that the 6p states are non-magnetic, and we consider only non-spin-flip scattering. Here we derive the T matrix for a generic l state, and at the end set $l = 1$ for Bi impurities in Cu.

$$T^{s-o}_{\mathbf{k}'\sigma,\mathbf{k}\sigma} = \langle \mathbf{k}'\sigma | V_{\rm mix} G V_{\rm mix} | \mathbf{k}\sigma \rangle = \sum_{j'm',jm} \langle \mathbf{k}'\sigma | V_{\rm mix} | j'm' \rangle \langle j'm' | G | jm \rangle \langle jm | V_{\rm mix} | \mathbf{k}\sigma \rangle \tag{13}$$

where

$$\langle jm | V_{\rm mix} | \mathbf{k}\sigma \rangle = \sum_{m''} \langle jm | lm''\sigma \rangle \langle lm''\sigma | V_{\rm mix} | \mathbf{k}\sigma \rangle,$$
$$\langle j'm' | G | jm \rangle = -\frac{1}{\Delta_j} e^{i\eta_j} \sin\eta_j \delta_{j',j} \delta_{m',m} \tag{14}$$

G is the propagator, Greens function, for a localized state which we assume is in spin–orbit quantized j states, and $\langle jm | lm''\sigma \rangle$ is a Clebsch–Gordan coefficient. This form for writing the T matrix, see Eq. (13), makes its relation to Friedel's vbs clear: a conduction electron hops onto a localized orbital, senses the SOC, and then hops off, i.e.,

$$\langle lm''\sigma | V_{\rm mix} | \mathbf{k}\sigma \rangle = \langle lm'' | V_{\rm mix} | klm'' \rangle \langle klm''\sigma | \mathbf{k}\sigma \rangle = \frac{V_k}{\sqrt{N_s}} \cdot i^l \sqrt{4\pi} Y_l^{m''*}(\hat{k}) \tag{15}$$

where V_k represents the isotropic mixing between a localized $l[p]$ state and the lth component of a plane wave state introduced by Anderson [19]. The V_k is related to Δ, the width of the virtual bound j states by, $\frac{|V_k|^2}{N_s} = \frac{\Delta}{\pi n(\varepsilon_{\rm F})}$, where N_s is the number of sites in the lattice. The phase shifts η_j describing the scattering is related to the specifics of the local orbital and the s-d mixing interaction from the definition of the phase shifts $\cot(\eta_j) = \frac{E_j - \epsilon_{\rm F}}{\Delta_j}$; see Ref. [8]. The spin–orbit coupling appears in the difference in energy of the levels $E_{l\pm\frac{1}{2}}$; a good picture of this can be found in one of our papers [20].

By including ordinary charge scattering, our complete T matrix for non-spin flip scattering is written as [4]

$$T_{\mathbf{k}'\sigma,\mathbf{k}\sigma} = \frac{2}{n(\varepsilon_{\rm F})} \left[\sum_{j=l\pm\frac{1}{2}} (2j+1) e^{i\eta_j} \sin\eta_j X(l,j) \right] \sigma \sum_m m Y_l^{m*}(\hat{k}) Y_l^m(\hat{k}')$$
$$- \frac{4}{n(\varepsilon_{\rm F})} \sum_{l,m} e^{i\eta_l} \sin\eta_l Y_l^{m*}(\hat{k}) Y_l^m(\hat{k}') \tag{16}$$

where $X(l,j) = \frac{\left[\frac{3}{4} + l(l+1) - j(j+1)\right]}{l\cdot(l+1)\cdot(2l+1)}$.

The first term is spin-dependent and antisymmetric when interchanging k and k', i.e., it contributes to $T_{\rm antisym}$, while the second is symmetric and contributes to $T_{\rm sym}$. To illustrate the use of this T matrix we use the example of Bi in Cu which we recently published [4], where we found

$$T_{\mathbf{k}'\sigma,\mathbf{k}\sigma}(\sigma = \uparrow\downarrow \to \pm) = \frac{4\sigma}{3n(\varepsilon_{\rm F})} \left(e^{i\eta_{1/2}} \sin\eta_{1/2} - e^{i\eta_{3/2}} \sin\eta_{3/2} \right) \sum_m m Y_1^{m*}(\hat{k}) Y_1^m(\hat{k}') - \frac{1}{\pi n(\varepsilon_{\rm F})} e^{i\eta_0} \sin\eta_0 \tag{17}$$

where we considered the dominant scattering is in the $l = 1$ channel (zero 6p states from Cu and about 3 for Bi) and a significant amount in $l = 0$ (1s state from Cu and 2 from Bi). Note that $\frac{2}{3}\left(e^{i\eta_{1/2}} \sin\eta_{1/2} - e^{i\eta_{3/2}} \sin\eta_{3/2}\right)$ can be rewritten as $\frac{1}{3i}\left(e^{i2\eta_{1/2}} - e^{i2\eta_{3/2}}\right)$. By placing this T matrix in Eqs. (12) and (10), we find that the spin-dependent contribution to the Hall resistivity is

$$\rho_H^{\rm skew}|_{\rm Fert} = \mp \frac{\frac{8}{3}\pi N_i \hbar}{n_\sigma e^2 k_{\rm F}} \sin\eta_0 \left[\sin\eta_{1/2} \sin(\eta_{1/2} - \eta_0) - \sin\eta_{3/2} \sin(\eta_{3/2} - \eta_0) \right] \tag{18}$$

where $\mp$ refers to the two directions of the electron spin.

In the limit of weak spin–orbit coupling, the difference in energy of the levels $E_{j=l\pm\frac{1}{2}} = E_l + \lambda_l \langle l \cdot s \rangle |_{l\pm\frac{1}{2}}$, which for $l = 1$ yields $E_{3/2} = E_{\rm p} + 1/2\lambda_p$, and $E_{1/2} = E_{\rm p} - \lambda_p$. By placing these energies in the definition of the phase shifts $\cot(\eta_j) = \frac{E_j - \epsilon_{\rm F}}{\Delta_j}$ (see Ref. [8]), we arrive at the weak spin–orbit coupling result

$$\eta_{1/2} = \eta_1 + \frac{\lambda_p}{\Delta} \sin^2\eta_1$$
$$\eta_{3/2} = \eta_1 - \frac{1}{2}\frac{\lambda_p}{\Delta} \sin^2\eta_1 \tag{19}$$

where η_1 is the mean phase shift at the Fermi level expressed as a function of the number $Z_{\rm p}$ of 6p electrons on the impurity by Friedel's sum rule, $\eta_1 = (2\eta_{3/2} + \eta_{1/2})/3 = \pi Z_{\rm p}/6$, see Ref. [8], in the limit of weak spin–orbit coupling. The

spin orbit coupling appears as the difference in energy of the levels $E_{j=l\pm\frac{1}{2}} = E_l + \lambda_l \langle l\cdot s\rangle|_{l\pm\frac{1}{2}}$; for $l=1$, this yields $E_{3/2} = E_p + 1/2\lambda_p$, and $E_{1/2} = E_p - \lambda_p$. By placing these energies in the definition of the phase shifts $\cot(\eta_j) = \frac{E_j-\epsilon_F}{\Delta_j}$, we arrive at the weak spin–orbit coupling result

$$\eta_{1/2} = \eta_1 + \frac{\lambda_p}{\Delta}\sin^2\eta_1$$
$$\eta_{3/2} = \eta_1 - \frac{1}{2}\frac{\lambda_p}{\Delta}\sin^2\eta_1 \tag{20}$$

where η_1 is the mean phase shift at the Fermi level expressed as a function of the number Z_p of 6p electrons on the impurity by Friedel's sum rule, $\eta_1 = (2\eta_{3/2} + \eta_{1/2})/3 = \pi Z_p/6$, see Ref. [8]. Upon placing these results in Eq. (18), we reproduce the spin-dependent transverse resistivity due to skew scattering originally found by Fert [16].

3.2. Side jump

Recently attention has been placed on a second contribution to the SHE, arising from the side jump or anomalous velocity. There is no formula as Eq. (10), which relates its contribution to the transverse resistivity in terms of a transition probability. Some work has related this contribution to a geometrical Berry phase acquired due to the SOC and a new interpretation of the anomalous Hall conductivity in terms of Berry phases [21]; also one has evaluated this contribution using the Kubo–Středa formula [2]. Here we review the approach we recently used for the side jump contribution to the SHE induced by Bi impurities in Cu [4]; this approach relies on the phase shifts introduced by Friedel and uses the scattering T matrix we have derived, see Eq. (17). We will not discuss the contribution arising from the SOC due to band structure inasmuch as this does not depend on scattering or a phase shift analysis.

The side jump contribution to the Hall resistivity is [4],

$$\rho_{yx}^{\text{side-jump}} = \frac{6}{e^2}\frac{\omega_a(k_F\sigma)}{n(\varepsilon_F)\upsilon_F^3\tau_o(k_F\sigma)} \tag{21}$$

where $\omega_a(k_F\sigma)$ is the anomalous velocity acquired by electrons in the presence of SOC on the scattering sites. This is given in terms of the scattering T matrix as [18],

$$\omega_a(\mathbf{k},\sigma) = \frac{2N_i}{\hbar}[\mathrm{Re}\,\nabla_{\mathbf{k}}T_{\mathbf{k}\sigma,\mathbf{k}\sigma} + \sum_{\mathbf{k}'\sigma'}P\frac{1}{(\varepsilon_{k\sigma}-\varepsilon_{k'\sigma'})}\mathrm{Re}\,T^{\dagger}_{\mathbf{k}\sigma,\mathbf{k}'\sigma'}\nabla_{\mathbf{k}'}T_{\mathbf{k}'\sigma',\mathbf{k}\sigma}$$
$$-\pi\sum_{\mathbf{k}'\sigma'}\delta(\varepsilon_{k\sigma}-\varepsilon_{k'\sigma'})\mathrm{Im}T^{\dagger}_{\mathbf{k}\sigma,\mathbf{k}'\sigma'}\nabla_{\mathbf{k}'}T_{\mathbf{k}'\sigma',\mathbf{k}\sigma}] \tag{22}$$

Only the last term contributes to the Hall effect, which we find by taking the gradient of Eq. (17); the procedure to carry this out is detailed in Ref. [22]. Our result for the anomalous velocity for 6p states is,

$$\omega_a(\mathbf{k},\sigma) = -\frac{2}{3}\sigma\frac{N_i}{\pi\hbar n(\varepsilon_F)}\sin\eta_0\times\left\{\begin{array}{c}\cos(2\eta_{1/2}-\eta_0)\partial_k\eta_{1/2} - \cos(2\eta_{3/2}-\eta_0)\partial_k\eta_{3/2}\\ +1/k_F\left[\sin(2\eta_{1/2}-\eta_0)-\sin(2\eta_{3/2}-\eta_0)\right]\end{array}\right\} \tag{23}$$

By placing the expressions for $\omega_a(k_F\sigma)$ and by using

$$\tau_0^{-1}(k_F\sigma) = \frac{2N_i}{\pi\hbar n(\varepsilon_F)}[\sin^2\eta_0 + 3\sin^2\eta_1] \tag{24}$$

in Eq. (21), we find that the side jump contribution to the Hall effect is

$$\rho_{yx}^{\text{side jump}}(\sigma=\uparrow\downarrow\to\pm) = \mp\frac{32}{9}\frac{N_i\hbar}{n_\sigma e^2}\frac{c}{z}\sin\eta_0[\sin^2\eta_0 + 3\sin^2\eta_1]$$
$$\times\left\{\begin{array}{c}\cos(2\eta_{1/2}-\eta_0)\partial_k\eta_{1/2} - \cos(2\eta_{3/2}-\eta_0)\partial_k\eta_{3/2}\\ +1/k_F\left[\sin(2\eta_{1/2}-\eta_0)-\sin(2\eta_{3/2}-\eta_0)\right]\end{array}\right\} \tag{25}$$

where c is the impurity concentration, and $z \equiv \frac{n_{\text{total}}}{N_s} = \frac{2n_\sigma}{N_s}$, i.e., the number of conduction electrons per lattice site.

To obtain the side-jump contribution to the Hall resistivity in the limit of weak spin–orbit coupling, i.e., to first order in the difference in the phase shifts $\Delta\eta$, we use $\eta_{1/2} = \eta_1 + 2/3\Delta\eta$, and $\eta_{3/2} = \eta_1 - 1/3\Delta\eta$. These expressions are derived from the definitions for $\Delta\eta \equiv \eta_{1/2} - \eta_{3/2}$ and η_1 (see Eq. (19)), and we also use $\partial_k\eta|_{\varepsilon_F} = \frac{2E_F}{k_F}\partial_\varepsilon\eta|_{\varepsilon_F}$. With these relations, we find the term in curly brackets in Eq. (25), is to first order in $\Delta\eta$

$$\left\{\begin{array}{c}\cos(2\eta_{1/2}-\eta_0)\partial_k\eta_{1/2}-\cos(2\eta_{3/2}-\eta_0)\partial_k\eta_{3/2}\\ +1/k_F\left[\sin(2\eta_{1/2}-\eta_0)-\sin(2\eta_{3/2}-\eta_0)\right]\end{array}\right\}$$
$$\Rightarrow \Delta\eta\left\{\frac{2}{\sin\eta_1}\partial_k\eta_1\cos(3\eta_1-\eta_0)+\frac{2}{k_F}\cos(2\eta_1-\eta_0)\right\} \quad (26)$$

With these expressions, Eq. (25) reduces to,

$$\rho_{xy}^{\text{side-jump}}(\sigma=\uparrow\downarrow\rightarrow\pm)\Rightarrow\mp\frac{32}{9}\frac{N_i\hbar}{n_\sigma e^2}\frac{c}{z}\Delta\eta\sin\eta_0[\sin^2\eta_0+3\sin^2\eta_1]$$
$$\times\left\{\frac{2}{\sin\eta_1}\partial_k\eta_1\cos(3\eta_1-\eta_0)+\frac{2}{k_F}\cos(2\eta_1-\eta_0)\right\} \quad (27)$$

In the case that we can treat, the $l=1$ state as a resonant state, the derivative $\partial_k\eta|_{\varepsilon_F}=\frac{2E_F}{k_F}\partial_\varepsilon\eta|_{\varepsilon_F}$ reduces to $\frac{2E_F}{k_F}\frac{\sin^2\eta}{\Delta}$, where Δ is the width of the resonant state, so that $\rho_{xy}^{\text{side-jump}}$ is written as

$$\rho_{xy}^{\text{side-jump}}(\sigma=\uparrow\downarrow\rightarrow\pm)\Rightarrow\mp\frac{32}{9}\frac{N_i\hbar}{n_\sigma e^2k_F}\frac{c}{z}\Delta\eta\sin\eta_0[\sin^2\eta_0+3\sin^2\eta_1]$$
$$\times\left\{\frac{4E_F}{\Delta}\sin\eta_1\cos(3\eta_1-\eta_0)+2\cos(2\eta_1-\eta_0)\right\} \quad (28)$$

4. Reflection on Friedel's work

Jacques Friedel's thesis work has had a remarkable effect on the way we describe scattering of conduction electrons from impurities in metals. His concept of the vbs with the use of the phase shifts to describe the scattering has given rise to an extensive literature over the past sixty years. As we have shown, it is currently used in the study of the SHE. It has also led to the prediction of chiral spin interactions acting on magnetic films deposited on heavy metals and inducing topological magnetic solitons intensively studied nowadays and called skyrmions. It is amazing to see the recent increase of theoretical publications using a phase shift analysis of scattering effects and one of us (AF) has also been nicely surprised by several requests of the "polycopiés des cours de Friedel" that he had kept from the time he was following Friedel's lectures. What is also amazing is to see that some recent uses of the theoretical concepts introduced by Friedel a long time ago will probably soon lead to technological applications. For example, the new type of magnetic memory called SOT–MRAM (for Spin–Orbit Torque–Magnetic Random-Access Memory) has a writing process based on the SHE, and the first demonstration of this device in a Japanese laboratory [23] uses the large SHE of CuIr alloys predicted by a vbs model of Ir impurities in Cu [4]. Jacques Friedel would be happy to see the many bridges between his concepts of the 1960s and the most advanced devices of today's or tomorrow's technologies.

References

[1] J. Friedel, Philos. Mag. 43 (1952) 153.
[2] M. Gradhand, D.V. Fedorov, P. Zahn, I. Mertig, Phys. Rev. Lett. 104 (2010) 186403;
M. Gradhand, D.V. Fedorov, P. Zahn, I. Mertig, Phys. Rev. B 81 (2010) 245109;
S. Lowitzer, M. Gradhand, D. Ködderitzsch, D.V. Fedorov, I. Mertig, H. Ebert, Phys. Rev. Lett. 106 (2011) 056601;
M. Gradhand, D.V. Fedorov, P. Zahn, I. Mertig, Solid State Phenom. 168–169 (2011) 27;
K. Tauber, M. Gradhand, D.V. Fedorov, I. Mertig, Phys. Rev. Lett. 109 (2012) 026601;
C. Herschbach, M. Gradhand, D.V. Fedorov, I. Mertig, Phys. Rev. B 85 (2012) 195133;
D.V. Fedorov, C. Herschbach, A. Johansson, S. Ostanin, I. Mertig, M. Gradhand, K. Chadova, D. Ködderitzsch, H. Ebert, Phys. Rev. B 88 (2013) 085116.
[3] T. Seki, et al., Nat. Mater. 7 (2008) 125;
G.Y. Guo, S. Maekawa, N. Nagaosa, Phys. Rev. Lett. 102 (2009) 036401;
Bo Gu, Jing-Yu Gan, Nejat Bulut, Timothy Ziman, Guang-Yu Guo, Naoto Nagaosa, Sadamichi Maekawa, Phys. Rev. Lett. 105 (2010) 086401;
X. Wang, J. Xiao, A. Manchon, S. Maekawa, Phys. Rev. B 87 (2013) 081407(R).
[4] A. Fert, P.M. Levy, Phys. Rev. Lett. 106 (2011) 157208;
Peter M. Levy, H.X. Yang, M. Chshiev, Albert Fert, Phys. Rev. B 88 (2013) 214432.
[5] A. Fert, Peter M. Levy, Phys. Rev. Lett. 44 (1980) 1538;
P.M. Levy, A. Fert, Phys. Rev. B 23 (1980) 4667.
[6] S. Heinze, et al., Nat. Phys. 7 (2011) 713.
[7] S. Lounis, et al., Phys. Rev. Lett. 108 (2012) 207202;
L. Petersen, et al., Phys. Rev. B 73 (2006) 035325.
[8] E. Daniel, J. Friedel, in: J. Daunt, P. Edwards, F. Milford, M. Yaqub (Eds.), Proceedings of the Ninth International Conference on Low Temperature Physics, Columbus, Ohio, 1964, Plenum, New York, 1965, p. 933.
[9] The derivation of Eq. (6) and details of the calculations is given in Ref. [5].
[10] Higher-order terms in $1/R$ enter $E^{(3)}$, as, for example, ones proportional to $(R_A R_B)^{-2}$, but for large R, Eq. (8) is the leading term.
[11] A. Fert, Mater. Sci. Forum 59–60 (1990) 439.
[12] S. Heinze, et al., see Ref. [6]. H. Yang, et al., arXiv:1501.05511.
[13] A. Fert, et al., Nat. Nanotechnol. 8 (2013) 152.

[14] A. Thiaville, et al., Europhys. Lett. 100 (2012) 57002;
Emori, et al., Nat. Mater. 12 (2013) 611.
[15] M.I. Dyakonov, V.I. Perel, Pis'ma Zh. Eksp. Teor. Fiz. 13 (1971) 657, JETP Lett. 13 (1971) 467, Phys. Lett. A 35 (1971) 459.
[16] A. Fert, A. Friederich, A. Hamzic, J. Magn. Magn. Mater. 24 (1981) 231, see Sec. 5.
[17] A. Messiah, Quantum Mechanics, North-Holland, Amsterdam, 1961.
[18] P.M. Levy, Phys. Rev. B 38 (1988) 6779.
[19] P.W. Anderson, Phys. Rev. l24 (1961) 41.
[20] A. Fert, P.M. Levy, Phys. Rev. Lett. 106 (2011) 157208, see inset on Fig. 1.
[21] N.A. Sinitsyn, J. Phys. Condens. Matter 20 (2008) 023201.
[22] See Ref. [18], in particular see Eq. (3.2b). Also see D.M. Brink, G.R. Satchler, Angular Momentum, 2nd ed., Oxford University Press, Oxford, 1975, in particular p. 148 for the spherical tensor notation of vectors, p. 150 for the gradient formula, and pp. 136–144 for orthogonality and recoupling relations for the $3j$ symbols.
[23] M. Yamanouchi, L. Chen, J. Kim, M. Hayashi, H. Sato, S. Fukami, S. Ikeda, F. Matsukura, H. Ohno, Appl. Phys. Lett. 102 (2013) 022407.